1: M.p. > 300 °C; IR (Nujol): $\tilde{\nu}$ = 1261, 1208, 1191, 1101, 1020, 974, 839, 800, 721, 686 cm^{-1}; ^{1}H NMR (400 MHz, C_6D_6): $\delta = -0.42$ (18H, s, $AlCH_3$), 1.08 (54H, d, J = 17.4 Hz, $C(CH_3)_3$); ^{31}P NMR (162 MHz, C_6D_6): δ = 13.4; MS (EI, 70 eV): m/z = 1053 ([M^+ − Me], 100 %); elemental analysis calcd for $C_{30}H_{72}Al_6O_{18}P_6$ (1068.6): C 33.74, H 6.80, P 17.40; found: C 33.64, H 6.74, P 17.86.

2: M.p. 192 – 195 °C; IR (Nujol): $\tilde{\nu}$ = 1261, 1208, 1190, 1097, 1021, 870, 801, 722, 688 cm^{-1}; ^{1}H NMR (200 MHz, C_6D_6): $\delta = -0.31$ (12H, s, $AlCH_3$), 1.03 (36H, d, J = 17.5 Hz, $C(CH_3)_3$); ^{31}P NMR (101 MHz, C_6D_6): δ = 17.5; MS (EI, 70 eV): m/z = 697 ([M^+ − Me], 100 %); elemental analysis calcd for $C_{20}H_{48}Al_4O_{12}P_4$ (712.4): C 33.74, H 6.80; found: C 33.42, H 6.88.

Received: July 18, 1997 [Z 10697 IE]
German version: *Angew. Chem.* **1998**, *110*, 101 – 103

Keywords: aluminum · phosphonates · structure elucidation · zeolite analogues

[1] S. T. Wilson, B. M. Lok, C. A. Messina, T. R. Cannan, E. M. Flanigen, *J. Am. Chem. Soc.* **1982,** *104*, 1146.
[2] M. Estermann, L. B. McCusker, C. Baerlocher, A. Merrouche, H. Kessler, *Nature* **1991**, *352*, 320.
[3] a) A. M. Chippindale, R. I. Walton, *J. Chem. Soc. Chem. Commun.* **1994**, 2453; b) R. H. Jones, A. M. Chippindale, S. Natarajan, J. M. Thomas, *ibid.* **1994**, 565.
[4] a) X. Yin, L. F. Nazar, *J. Chem. Soc. Chem. Commun.* **1994**, 2349; b) S. Oliver, A. Kuperman, A. Lough, G. A. Ozin, *Inorg. Chem.* **1996**, *35*, 6373.
[5] a) M. E. Davis, *Acc. Chem. Res.* **1993**, *26*, 111; b) *Ind. Eng. Chem. Res.* **1991**, *30*, 1675.
[6] Y. Yang, H.-G. Schmidt, M. Noltemeyer, J. Pinkas, H. W. Roesky, *J. Chem. Soc. Dalton. Trans.* **1996**, 3609.
[7] M. G. Walawalkar, R. Murugavel, A. Voigt, H. W. Roesky, H.-G. Schmidt, *J. Am. Chem. Soc.* **1997**, *119*, 4656.
[8] M. G. Walawalkar, R. Murugavel, A. Voigt, H. W. Roesky, H.-G. Schmidt, *Organometallics* **1997**, *16*, 516.
[9] K. Dimert, U. Englert, W. Kuchen, F. Sandt, *Angew. Chem.* **1997**, *109*, 251; *Angew. Chem. Int. Ed. Engl.* **1997**, *36*, 241.
[10] M. R. Mason, M. S. Mashuta, J. F. Richardson, *Angew. Chem.* **1997**, *109*, 239; *Angew. Chem. Int. Ed. Engl.* **1997**, *36*, 239.
[11] A. Keys, S. Bott, A. R. Barron, *Chem. Commun.* **1996**, 2339.
[12] M. R. Mason, R. M. Matthews, M. S. Mashuta, J. F. Richardson, *Inorg. Chem.* **1996**, *35*, 5756.
[13] W. M. Meier, D. H. Oslon, C. Baerlocher, *Atlas of Zeolite Structure Types*, 4th ed., Elsevier, London, **1996**.
[14] S. H. Metzger, O. H. Basedow, A. F. Isbell, *J. Org. Chem.* **1964**, *29*, 627.
[15] Crystal data for **1**: $C_{30}H_{72}Al_6O_{18}P_6$, M_r = 1068.58, triclinic, space group $P\bar{1}$, a = 9.780(3), b = 13.228(3), c = 13.692(3) Å, α = 117.56(3), β = 97.68(3), γ = 103.51(3)°, V = 1465.5(5) Å^3, Z = 1, ρ_{calcd} = 1.211 g cm^{-3}, 3846 independent reflections, $R1$ = 0.0342 for $I > 2\sigma(I)$, $wR2$ = 0.0897 for all data. The data were collected on a Stoe-Siemens-AED2 four-circle diffractometer equipped with graphite-monochromated $Mo_{K\alpha}$ radiation (λ = 0.71073 Å). The measurements were made with the Learnt Profile Method on a cooled crystal coated with a drop of oil.[16] The structures were solved by direct methods (SHELXS-90)[17] and refined with all data by full-matrix least squares on F^2.[18] All non-hydrogen atoms were refined anisotropically. Hydrogen atoms were added in idealized positions and included in the refinement. Crystallographic data (excluding structure factors) for the structure reported in this paper have been deposited with the Cambridge Crystallographic Data Centre as supplementary publication no. CCDC-100575. Copies of the data can be obtained free of charge on application to CCDC, 12 Union Road, Cambridge CB2 1EZ, UK (fax: int. code + (44)-1223 336-033; e-mail: deposit@ccdc.cam.ac.uk).
[16] W. Clegg, *Acta Crystallogr. Sect. A* **1981**, *37*, 22.
[17] G. M. Sheldrick, *Acta Crystallogr. Sect. A* **1990**, *46*, 467.
[18] G. M. Sheldrick, SHELXL-93, *Program for Crystal Structure Refinement*, Universität Göttingen, **1993**.
[19] a) A. Simmen, L. B. McCusker, C. Baerlocher, W. M. Meier, *Zeolites* **1991**, *11*, 654; b) N. K. Mcguire, C. A. Bateman, C. S. Blackwell, S. T. Wilson, R. M. Kirchner, *ibid.* **1995**, *15*, 460; c) B. M. Lok, C. A. Messina, R. L. Patton, R. T. Gajek, T. R. Cannan, E. M. Flanigen, *J. Am. Chem. Soc.* **1984**, *106*, 6092.

The Mechanism for Hydrogen Abstraction by n,π* Excited Singlet States: Evidence for Thermal Activation and Deactivation through a Conical Intersection**

Werner M. Nau,* Gerhard Greiner,* Julia Wall, Hermann Rau, Massimo Olivucci,* and Michael A. Robb

Salem's correlation diagram for hydrogen abstraction by n,π* excited chromophores,[1] most often depicted for the reaction between formaldehyde and methane, has become the classic textbook example for a theoretical rationalization of photochemical reactivity and for the contrast between the reactivity of singlet and triplet states. According to this diagram the hydrogen abstraction by triplet states proceeds smoothly and with unit efficiency, whereas for singlet states the system is predicted to "pause" at an avoided crossing and then to proceed either to the products or back to the reactants; this reduces the efficiency to below unity.[1,2] While the triplet reaction has received considerable experimental and theoretical attention, the distinct singlet mechanism has not been examined in detail.[3–6]

The intermolecular hydrogen abstraction of the n,π* excited singlet states of ketones is difficult to examine owing to short lifetimes and efficient intersystem crossing. This limitation warrants the choice of an alternative n,π* chromophore. The azoalkane 2,3-diazabicyclo[2.2.2]oct-2-ene (DBO) appeared to be the predestined experimental test case, since excited singlet DBO is very long-lived (up to 1 μs) and undergoes neither intersystem crossing[7] nor efficient photodecomposition (only about 2 %).[8] Moreover, excited singlet azoalkanes are efficiently quenched by C–H and O–H bonds of poor hydrogen donors such as chloroform or methanol.[9–11] This provides a fascinating case of a singlet hydrogen abstraction [Eq. (1)], which we have now elucidated in mechanistic detail. An unexpectedly low activation barrier and a large deuterium isotope effect are observed for chloroform as hydrogen donor. These findings are rationalized in terms of a thermally activated rather than a tunneling process.

[*] Dr. W. M. Nau
Institut für Physikalische Chemie der Universität Basel
Klingelbergstrasse 80, CH-4056 Basel (Switzerland)
Fax: Int. code + (41) 61-267 3855
e-mail: nau@ubaclu.unibas.ch

Priz.-Doz. G. Greiner, J. Wall, Prof. H. Rau
Institut für Chemie der Universität Hohenheim
Garbenstrasse 30, D-70599 Stuttgart (Germany)
Fax: Int. code + (49) 711-459 3881
e-mail: greiner@uni-hohenheim.de

Dr. M. Olivucci
Dipartimento di Chimica "G. Ciamician" dell'Università
Via Selmi 2, 40126 Bologna (Italy)
Fax: Int. code + (39) 51-259456
e-mail: max@ciam.unibo.it

Prof. M. A. Robb
Department of Chemistry, King's College, London (UK)

[**] W.M.N. would like to thank the Fonds der Chemischen Industrie for a Liebig fellowship and Prof. J. C. Scaiano for helpful discussions. M.O. and M.A.R. are grateful to NATO for a travel grant and to Dr. Paolo Celani for help with the CAS computations.

  1433-7851/98/3701-0098 $ 17.50+.50/0

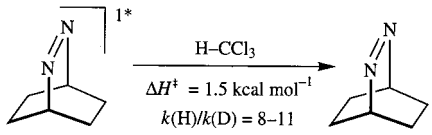

(1)

Most importantly, the computed reaction pathway for hydrogen abstraction from C–H bonds by excited singlet azoalkanes involves decay at a conical intersection (i. e., a real surface crossing)[12,13] of the excited- and ground-state energy sheets (Figure 1) rather than the previously implicated

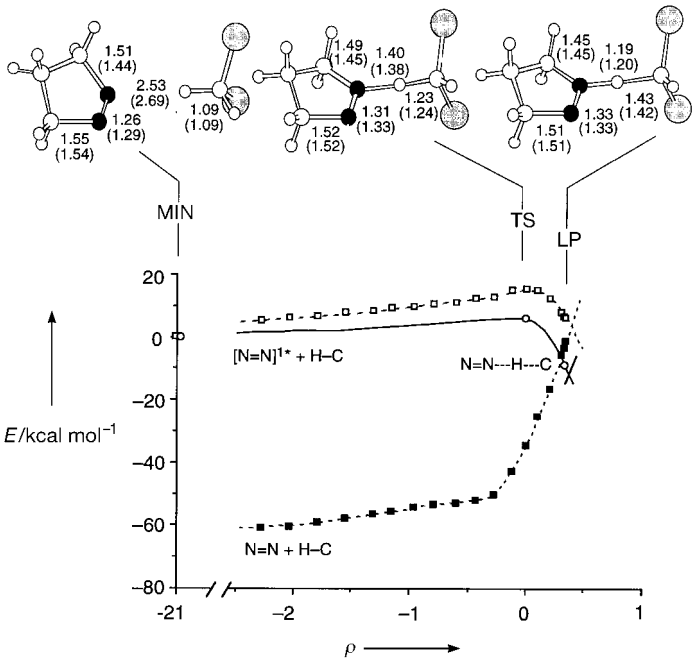

Figure 1. Energy profile along the S_1-(n,π*) reaction coordinate ρ [bohr (amu)$^{1/2}$] describing the hydrogen abstraction in the pyrazoline/CH_2Cl_2 system (see ref. [18] for computational details). Open and filled squares and the associated dashed lines indicate the relative CAS(8,7) energies of the S_1 and S_0 (CI values) states, respectively. Open circles and the solid line present the more accurate CAS(12,10)/PT2F energy profile for the S_1 state. The structures of MIN, TS, and LP [CAS(12,10) and (in parentheses) CAS(8,7) geometrical parameters in Å] document the geometrical progression along the reaction path. The LP point ($S_1 - S_0$ energy gap about 4 kcal mol^{-1}) is taken as representative of the conical intersection.

avoided crossing. The data lead us to propose a mechanism in which the deactivation of n,π* excited singlet azoalkanes is triggered by partial H abstraction from a solvent molecule loosely bound to a nitrogen center. In fact, the hydrogen abstraction on the excited-state surface is aborted at the conical intersection,[13] at which point the system must decay efficiently to the ground-state surface. The radiationless decay is experimentally manifested in low reaction quantum yields.

The decay rate of excited singlet DBO ($1/\tau$) can be analyzed as a composite of the rates of fluorescence (k_f), intramolecular radiationless deactivation (k_d), and intermolecular (solvent-induced) quenching (k_q)—that is, $1/\tau = k_f + k_d + k_q$. The gas-phase fluorescence lifetime[14,15] at ambient temperature (τ_0(DBO) = (930 ± 30) ns) is characteristic for conditions under which the latter process is absent ($1/\tau_0 = k_f + k_d$). In all common solvents, however, the fluorescence lifetime of DBO is shortened, whereas deuterated solvents display a smaller effect. Consequently, solvent-induced quenching (k_q) must be considered ($1/\tau = 1/\tau_0 + k_q$).

As previously corroborated by means of decomposition quantum yields,[9] most solvent-induced quenching of azoalkanes is chemically unproductive and results in radiationless deactivation; for DBO in nonprotic solvents the chemical reaction contributes less than 5%. Nevertheless, from the involvement of C–H bonds in the quenching process and the deuterium isotope effects we conclude that the solvent-induced deactivation must occur along the reaction coordinate for hydrogen abstraction, thus providing an example of an "aborted" hydrogen abstraction. This mechanistic interpretation of the experimental data is corroborated by our theoretical results (see Figure 1).

Chloroform as solvent was examined in experimental detail, since the observed quenching and isotope effects are amongst the largest (Table 1). The fluorescence lifetimes at ambient temperature (22–25 °C) were measured by three techniques (laser flash photolysis, single-photon counting, and streak camera detection) in different laboratories, and consistent results were obtained. The fluorescence quantum yields (Table 1) follow the same trend as the fluorescence lifetimes, and their ratio suggest a natural fluorescence lifetime (τ_n) of (1500 ± 300) ns, which is not significantly different from that in the gas phase (τ_n = (1700 ± 300) ns).[14] Most striking is that the fluorescence lifetime in chloroform is only (13 ± 1) ns, that is, nearly two orders of magnitude shorter than under conditions for which no intermolecular quenching applies (τ_0 = 930 ns). The use of the deuterated solvent ($CDCl_3$) increases the fluorescence lifetime by nearly one order of magnitude ((110 ± 5) ns). The calculated pseudo-unimolecular quenching rate constants k_q (Table 1) substantiate a deuterium isotope effect k_q(H)/k_q(D) of 8–11 at ambient temperature. This value exceeds the kinetic isotope effect expected from energy differences in C–H and C–D stretching vibrations alone (ca. 6), but lies at the upper limit when allowance for bending mode contributions is made (10).[16] This is the largest primary C–H/D isotope effect ever observed for an intermolecular photochemical hydrogen abstraction. For comparison, the isotope effects in the hydrogen abstraction by n,π* excited ketones range from 1–5.[3,4]

Table 1. Fluorescence lifetimes τ and quantum yields Φ for 2,3-diazabicyclo[2.2.2]oct-2-ene (DBO) as well as rate constants k_q and activation parameters for fluorescence quenching.

	Gas phase	$CHCl_3$	$CDCl_3$
τ/ns	930 ± 30 ($\equiv\tau_0$)	13 ± 1	110 ± 5
Φ	0.56 ± 0.10[a]	~0.01	0.075 ± 0.008
τ_n/ns[b]	1700 ± 300	~1300	1500 ± 250
$k_q/10^6$ s^{-1}		76 ± 6	8.0 ± 0.4
$A/10^9$ s^{-1}		2.3 ± 0.3	1.6 ± 0.3
E_A/kcal mol^{-1}		2.05 ± 0.07	3.15 ± 0.09
$\Delta S^{\neq}$/cal K^{-1} mol^{-1}		−17.6 ± 2.4	−18.3 ± 3.4
$\Delta H^{\neq}$/kcal mol^{-1}		1.50 ± 0.05	2.60 ± 0.07

[a] From ref. [14]. [b] Natural fluorescence lifetime ($\tau_n = \tau/\Phi$).

  1433-7851/98/3701-0099 $ 17.50+.50/0

The fluorescence lifetimes of DBO in $CHCl_3$ and $CDCl_3$ increase at lower temperatures and decrease upon heating, indicating a thermally activated process. The temperature dependence of the solvent-induced quenching ($k_q = 1/\tau - 1/\tau_0$)[17] was measured from -30 to $+50\,^{\circ}C$ by single-photon counting. The corresponding Arrhenius (Figure 2) or Eyring

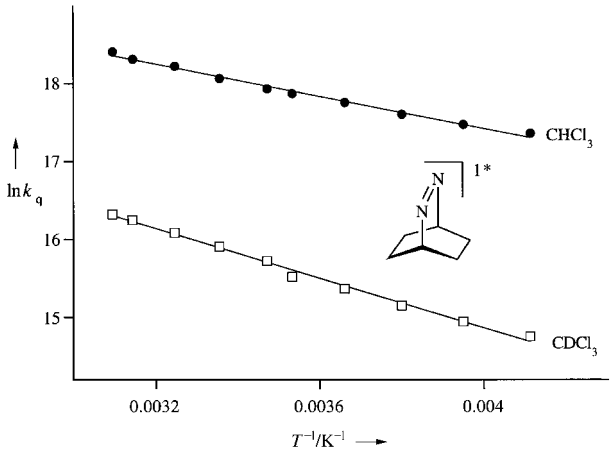

Figure 2. Arrhenius plots for the fluorescence quenching of DBO by $CHCl_3$ and $CDCl_3$ as solvents.

plots, which were linear in the examined temperature range ($r^2 > 0.99$), provide the activation parameters in Table 1. Most importantly, differences in the activation entropy ($\Delta S^{\neq}$) were insignificant, whereas the activation enthalpy ($\Delta H^{\neq}$) increased from 1.5 to 2.6 kcal mol^{-1} upon deuteration. This behavior suggests a classical kinetic isotope effect due to differences in the zero-point energy (ZPE).

The reaction pathway for the intermolecular hydrogen abstraction of an n,π* excited singlet azoalkane was established by ab initio methods.[18] A simpler model reaction, namely that between 1,2-diazacyclopent-1-ene (pyrazoline) and dichloromethane, was selected to allow the use of accurate but expensive computational methodology. It comprises the MCSCF calculation[19] and multireference Møller–Plesset perturbation theory (PT2F),[20] which provides excellent data when tested for other photochemical parameters of azoalkanes (Table 2), namely the 0–0 singlet excitation energy (GS MIN) and the activation energy for α-C–N bond cleavage (TS_α). The same level of theory successfully predicted virtually all experimental aspects of the solvent-induced deactivation of singlet excited azoalkanes, namely the low activation barriers, the isotope effects, and the high efficiency of radiationless deactivation at the expense of product formation.

The computed reaction pathway (see Figure 1) initiates at a loosely bound excited state complex (MIN) in which one of the two dichloromethane C–H bonds lies in the pyrazoline plane and points towards the nitrogen atom containing the "equatorial" unpaired electron; in this complex the geometry of pyrazoline corresponds to that of the isolated n,π* state. The reaction coordinate is initially dominated by the intermolecular distance. After shortening of the H–N distance from 2.5 to 1.6 Å the hydrogen transfer (i. e., simultaneous expansion of the C–H and contraction of the H–N distances) becomes important. Such motion is accompanied by expansion of the N–N bond and shortening of both C–N bonds of pyrazoline. After the transition state (TS) the energy decreases very rapidly. Remarkably, the reaction path does not end at a stationary point (as expected if the previously postulated avoided crossing took place)[1,9] but at a conical intersection (i.e., a singularity) between the excited- (S_1) and ground-state (S_0) potential energy surfaces. This intersection is located near the last calculated point (LP)[18] and about 6 kcal mol^{-1} below the initial complex and provides an extremely efficient channel for radiationless decay. Conceptually, the aborted hydrogen abstraction in Figure 1 presents an example of the minimum →transition state →conical intersection topology, which was documented for intramolecular photoreactions in polyenes and benzene.[13] In this particular topology, access to the radiationless decay channel is thermally controlled.

The energies (Table 2) and vibrational frequencies of the n,π* loosely bound complex and transition state provide a direct comparison of the computed (for the pyrazoline/CH_2Cl_2 model system) and experimentally measured (for DBO/$CHCl_3$) activation parameters. The computed activation enthalpy is 6.4 kcal mol^{-1} but becomes 2.9 kcal mol^{-1} when the ZPE correction is taken into account, and, thus, falls within 1.4 kcal mol^{-1} of the $\Delta H^{\neq}$ observed for the DBO/$CHCl_3$ system. The calculated activation enthalpy for monodeuterated dichloromethane is 0.95 kcal mol^{-1} higher as a consequence of ZPE differences, which is in good agreement with the experimental difference for chloroform (about 1.1 kcal mol^{-1}). Since the experimental and computed isotope effects are only manifested in enthalpic differences, tunneling does not seem to contribute significantly in the examined temperature range. Consequently, the photochemical hydrogen abstraction of excited singlet azoalkanes can be mecha-

Table 2. Calculated[a] and experimental energies for photochemical reactions of the S_1-(n,π*) state of pyrazoline/CH_2Cl_2, pyrazoline, and DBO.

System	Structure[b]	E [Hartree][c]	ΔE_{calcd}[d]	$\Delta E_{exp.}$[e]
pyrazoline/CH_2Cl_2	MIN (S_1)	−1184.97785 (0.73)	≡0.0	≡0.0
	TS (S_1)	−1184.96769 (0.73)	6.4 [2.9]	1.5–2.6[f]
	LP (S_1)[g]	−1184.98824 (0.73)	−6.5	
pyrazoline	GS MIN	−226.67300 (0.84)	−84.0 [−82.7]	−82[h]
	MIN (S_1)	−226.53910 (0.82)	≡0.0	≡0.0
	TS_α (S_1)	−226.52694 (0.82)	7.6 [6.4]	6–9[i]
DBO	GS MIN	−343.01729 (0.75)	−73.7	−76[h]
	MIN (S_1)	−342.89980 (0.74)	≡0.0	≡0.0
	TS_α (S_1)	−342.88167 (0.74)	11.4	8.6–10.2[j]

[a] The multireference Møller–Plesset (PT2F) level of theory was employed; see ref. [10] for details. [b] For the abbreviations MIN, TS, and LP see Figure 1; GS MIN: 0–0 singlet excitation energy, TS_α: activation energy for α-C–N bond cleavage. [c] Calculated absolute energy. The weight of the MCSCF reference function (zeroth-order function) in the first-order function is given in parentheses. [d] Calculated values in kcal mol^{-1}. ZPE-corrected values are given in square brackets. [e] Experimental values in kcal mol^{-1}. [f] Values for the DBO/$CHCl_3$ and DBO/$CDCl_3$ system determined in this work. [g] Last optimized point along the S_1 reaction coordinate. [h] From ref. [7]. [i] Value for a pyrazoline derivative.[22,23] [j] Values for DBO derivatives.[8,11]

  1433-7851/98/3701-0100 $ 17.50+.50/0 *Angew. Chem. Int. Ed.* **1998**, *37*, No. 1/2

nistically viewed as a thermally activated process, as previously established for many triplet ketones.[4,21]

In conclusion, the combined experimental and theoretical data for the solvent-induced quenching of n,π* excited singlet azoalkanes support a hydrogen abstraction in which a transition state is followed by a conical intersection as the reaction coordinate. This photochemical reaction mechanism should be general for n,π* singlet excited chromophores and provides an important rationale for their reactivity and efficiency in hydrogen abstractions.

Received: June 11, 1997 [Z 10537 IE]
German version: *Angew. Chem.* **1998**, *110*, 103 – 107

Keywords: ab initio calculations · azo compounds · hydrogen transfer · isotope effects · photochemistry

[1] L. Salem, C. Leforestier, G. Segal, R. Wetmore, *J. Am. Chem. Soc.* **1975**, *97*, 479 – 487.
[2] N. J. Turro, J. McVey, V. Ramamurthy, P. Lechtken, *Angew. Chem.* **1979**, *91*, 597 – 612; *Angew. Chem. Int. Ed. Engl.* **1979**, *18*, 572 – 586.
[3] W. M. Nau, F. L. Cozens, J. C. Scaiano, *J. Am. Chem. Soc.* **1996**, *118*, 2275 – 2282, and references therein.
[4] M. A. Garcia-Garibay, A. Gamarnik, R. Bise, L. Pang, W. S. Jenks, *J. Am. Chem. Soc.* **1995**, *117*, 10264 – 10275.
[5] D. Severance, H. Morrison, *Chem. Phys. Lett.* **1989**, *163*, 545 – 548.
[6] A. E. Dorigo, M. A. McCarrick, R. J. Loncharich, K. N. Houk, *J. Am. Chem. Soc.* **1990**, *112*, 7508 – 7514.
[7] P. S. Engel, D. W. Horsey, J. N. Scholz, T. Karatsu, A. Kitamura, *J. Phys. Chem.* **1992**, *96*, 7524 – 7535.
[8] P. S. Engel, D. W. Horsey, D. E. Keys, C. J. Nalepa, L. R. Soltero, *J. Am. Chem. Soc.* **1983**, *105*, 7108 – 7114.
[9] W. M. Nau, W. Adam, J. C. Scaiano, *Chem. Phys. Lett.* **1996**, *253*, 92 – 96.
[10] M. J. Mirbach, M. F. Mirbach, W. R. Cherry, N. J. Turro, P. Engel, *Chem. Phys. Lett.* **1978**, *53*, 266 – 269.
[11] P. S. Engel, C. J. Nalepa, *Pure Appl. Chem.* **1980**, *52*, 2621 – 2632.
[12] M. Klessinger, *Angew. Chem.* **1995**, *107*, 597 – 599; *Angew. Chem. Int. Ed. Engl.* **1995**, *34*, 549 – 551, and references therein.
[13] F. Bernardi, M. Olivucci, M. A. Robb, *Chem. Soc. Rev.* **1996**, 321 – 328.
[14] B. S. Solomon, T. F. Thomas, C. Steel, *J. Am. Chem. Soc.* **1968**, *90*, 2249 – 2258.
[15] H. Rau, *Angew. Chem.* **1973**, *85*, 248 – 258; *Angew. Chem. Int. Ed. Engl.* **1973**, *12*, 224 – 239.
[16] R. P. Bell, *The Tunnel Effect in Chemistry*, Chapman und Hall, London, **1980**.
[17] For the calculation of k_q the ambient-temperature value of τ_0 ((930 ± 30) ns, gas phase) was employed for all temperatures. Inclusion of the much smaller temperature dependence of τ_0, which implicitly includes any temperature dependence of k_f and k_d and the possible contribution due to photodecomposition, does not affect the activation parameters within the limits of statistical regression error. For comparison, the gas-phase lifetimes are 950 and 885 ns at −20 and 65 °C, respectively; that is, they are within the limits of error of or very close to the ambient value.
[18] All MCSCF geometry optimizations were carried out with a complete active space (CAS) including 12 electrons in 10 orbitals (CAS(12,10)). The CAS orbitals comprise the π and π* N=N orbitals, the four σ and σ* C–N orbitals, the two nitrogen lone pair orbitals of the pyrazoline fragment, and the σ and σ* orbitals of the reactive C–H bond of CH_2Cl_2. To improve the description of the H transfer the standard 6-31G* basis set (double-ζ + d-type polarization function for atoms of the first and seconds rows of the periodic system) was augmented with p-type polarization and s-type diffuse functions on the CH_2Cl_2 hydrogen atoms and with sp-type diffuse functions (included in Gaussian 94)[19b] on the nitrogen centers. To improve the energetics by including the effect of dynamic electron correlation, the S_1 energies of MIN, TS, and LP were recomputed using multireference Møller–Plesset perturbation theory with the PT2F method included in MOLCAS.[20] To reduce the computational cost we used a CAS(8,7) with the 6-31G* basis set for the reaction coordinate and frequency computations. This reduced CAS does not include the σ and σ* orbitals of the "short" C–N bond and the lone-pair orbital on the alternative N atom. CAS(8,7) produces optimized geometries of MIN, TS, and LP which differ only slightly from that of CAS(12,10) (see Figure 1, top). The reaction coordinate was determined with the IRC method available in Gaussian 94. The conical intersection is easily located by computing the reaction coordinate until degeneracy of S_1 and S_0 is achieved. This manifests itself in failure of the MCSCF calculation to converge owing to $S_1 - S_0$ near-degeneracy. The last reaction coordinate point before degeneracy (LP) is taken as representative of the conical intersection.
[19] a) B. O. Roos, *Adv. Chem. Phys.* **1987**, *69*, 399 – 446; b) the MCSCF program used is implemented in Gaussian 94, Revision B.2: M. J. Frisch, G. W. Trucks, H. B. Schlegel, P. M. W. Gill, B. G. Johnson, M. A. Robb, J. R. Cheeseman, T. Keith, G. A. Petersson, J. A. Montgomery, K. Raghavachari, M. A. Al-Laham, V. G. Zakrzewski, J. V. Ortiz, J. B. Foresman, C. Y. Peng, P. Y. Ayala, W. Chen, M. W. Wong, J. L. Andres, E. S. Replogle, R. Gomperts, R. L. Martin, D. J. Fox, J. S. Binkley, D. J. Defrees, J. Baker, J. P. Stewart, M. Head-Gordon, C. Gonzalez, J. A. Pople, Gaussian, Inc., Pittsburgh, PA, USA, **1995**.
[20] a) K. Andersson, P.-A. Malmqvist, B. O. Ross, *J. Chem. Phys.* **1992**, *96*, 1218 – 1226; b) MOLCAS, Version 3: K. Andersson, M. R. A. Blomberg, M. Fülscher, V. Kellö, R. Lindh, P.-A. Malmqvist, J. Noga, J. Olsen, B. O. Roos, A. J. Sadlej, P. E. M. Siegbahn, M. Urban, P. O. Widmark, University of Lund, Sweden, **1994**.
[21] P. J. Wagner, Q. Cao, R. Pabon, *J. Am. Chem. Soc.* **1992**, *114*, 346 – 348.
[22] P. S. Engel, L. R. Soltero, S. A. Baughman, C. J. Nalepa, P. A. Cahill, R. B. Weisman, *J. Am. Chem. Soc.* **1982**, *104*, 1698 – 1700.
[23] M. F. Mirbach, M. J. Mirbach, K.–C. Liu, N. J. Turro, *J. Photochem.* **1978**, *8*, 299 – 306.

Catalytic, Highly Regio- and Chemoselective Generation of Radicals from Epoxides: Titanocene Dichloride as an Electron Transfer Catalyst in Transition Metal Catalyzed Radical Reactions**

Andreas Gansäuer,* Marianna Pierobon, and Harald Bluhm

During the last two decades the development of efficient chain reactions has led to an explosive growth in free radical chemistry.[1] Although the understanding of how substrate control determines the stereo- and chemoselectivity of these reactions has reached a high level,[2] to the best of our knowledge little is known about reagent-controlled, catalytic transformations of radicals not proceeding as chain reactions.[3] The advantage of this type of reaction is broader application because the influence of the substrate on the chemo- and stereoselectivity can ideally be overruled and the course of the reaction determined solely by the reagent in catalytic amounts. Therefore a reagent-controlled catalytic reaction would extend the synthetic utility of free radicals even further.

[*] Dr. A. Gansäuer, M. Pierobon, H. Bluhm
Institut für Organische Chemie der Universität
Tammannstrasse 2, D-37077 Göttingen (Germany)
Fax: Int. code + (49) 551-392944
e-mail: agansae@gwdg.de

[**] This work was supported by the Fonds der Chemischen Industrie and the Socrates Program. We thank Prof. R. Brückner for constant support and encouragement.